

Evolution of Dendritic Extended 3D Patterns during Directional Solidification: Microgravity Experiments in DECLIC-DSI onboard ISS and Phase-field Modeling

*Kaihua Ji¹, F.L. Mota², T. Lyons¹, L.S. Littles³,
R. Trivedi⁴, N. Bergeon², A. Karma¹*



¹Northeastern University

²IM2NP, Aix-Marseille Université

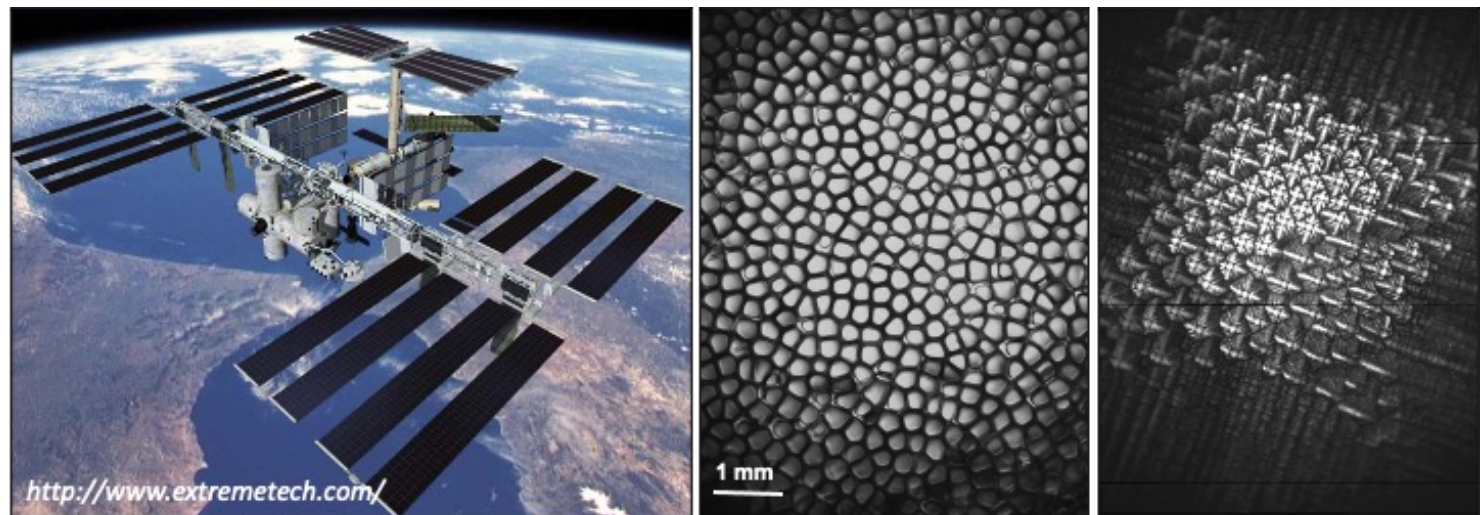
³Marshall Space Flight Center

⁴Iowa State University



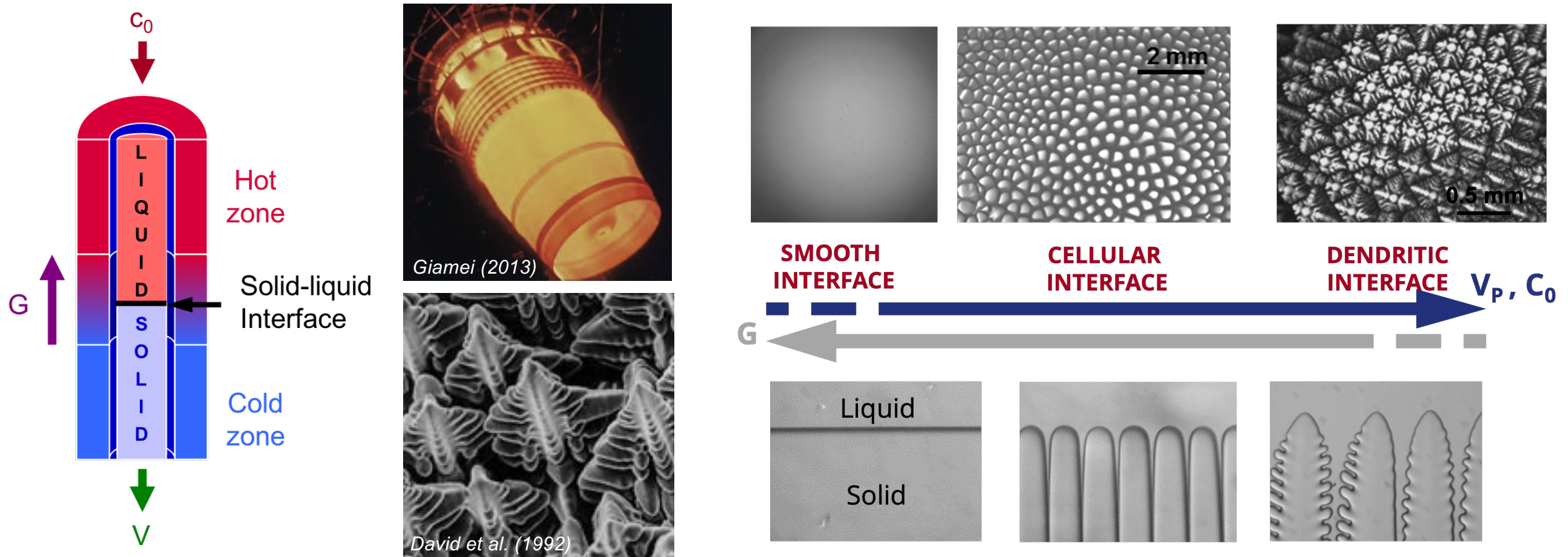
Outline

- Microgravity experiment: DEvice for the study of Critical LIquids and Crystallization - Directional Solidification Insert (DECLIC-DSI)
- Phase-field modeling
- DSI-R Campaign
 - Transient recoil and morphological instability
 - Dendrite tip radius measurements (using interferometry)
 - Curvature effects
- Summary and outlook



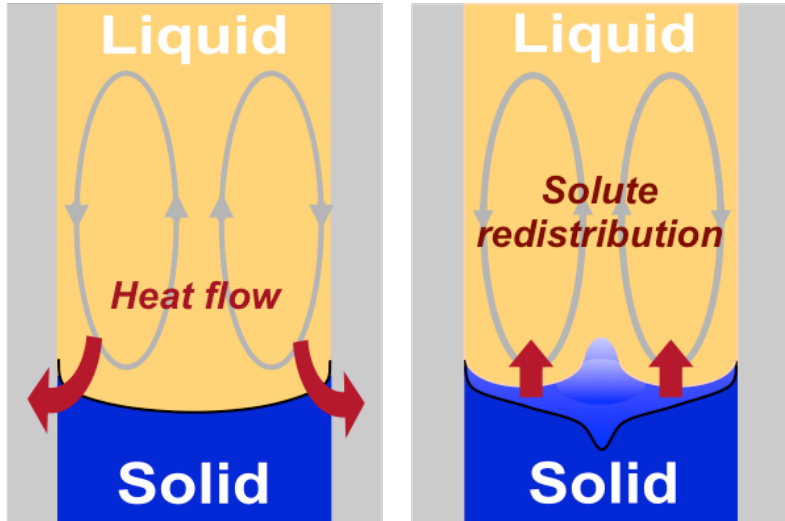
Directional solidification

- Microstructure formation under well-controlled growth conditions during directional solidification: alloy (solute) concentration C_0 , a constant pulling rate V_p , and a thermal gradient G .

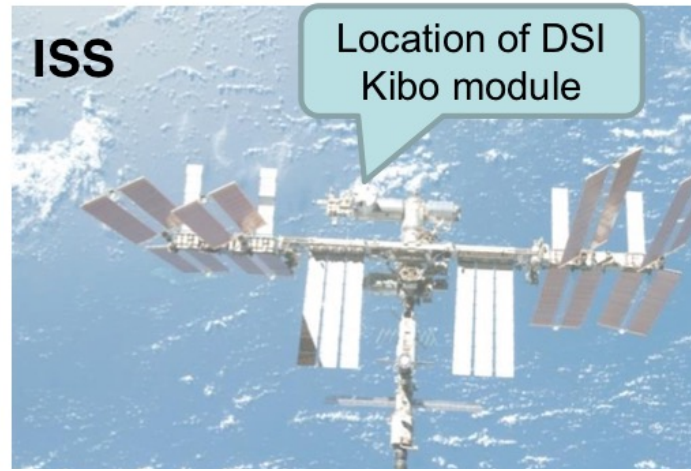


Microgravity experiments

Gravity-induced convection



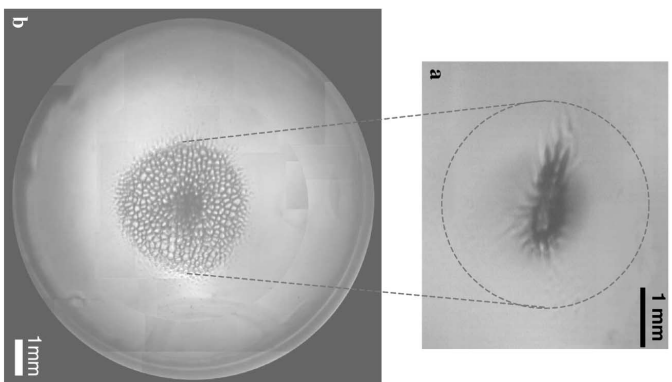
Microgravity experiment



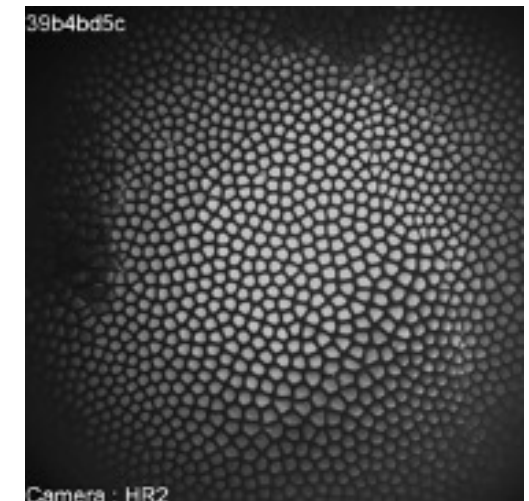
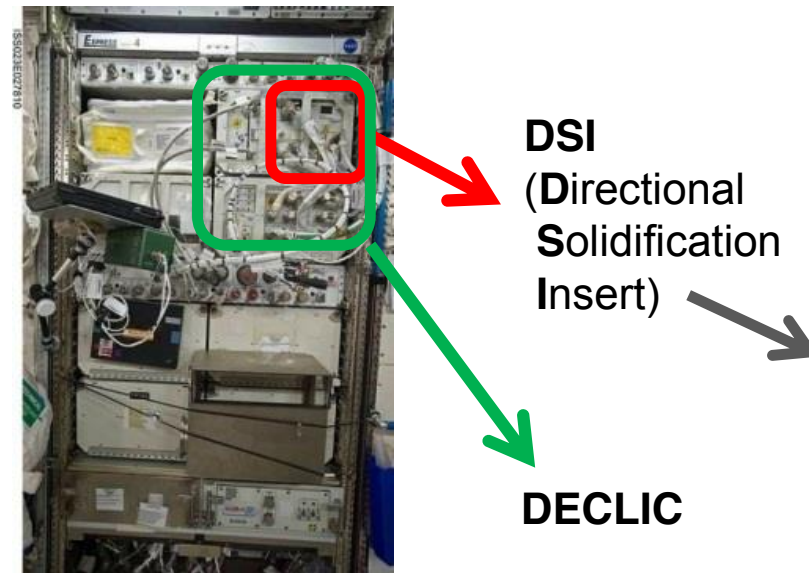
Two campaigns:

- 1) Microgravity experiments from **2009-2011** dedicated to cellular regime (**DSI**).
- 2) Microgravity experiments from **2017-2018** dedicated to dendritic regime (**DSI-R**).

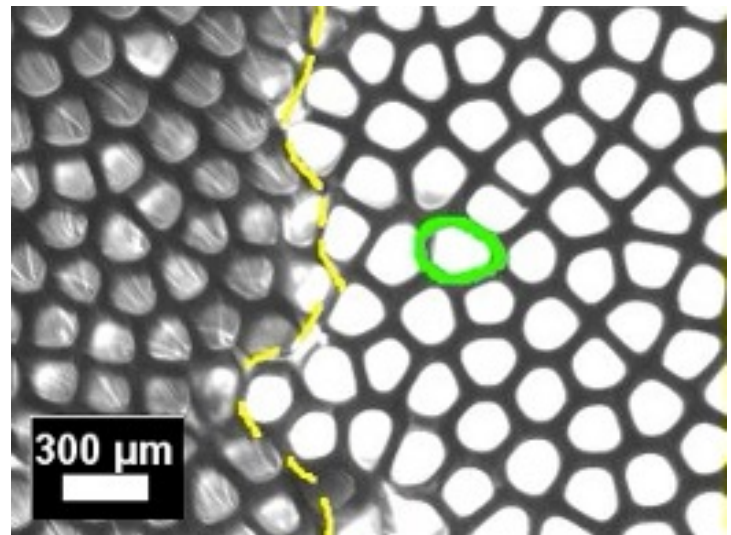
Microstructure heterogeneities



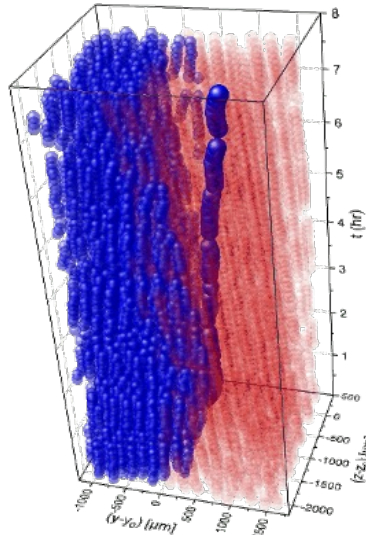
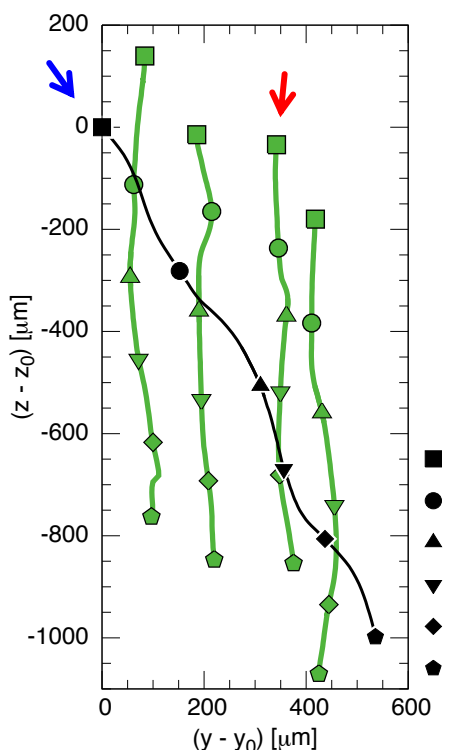
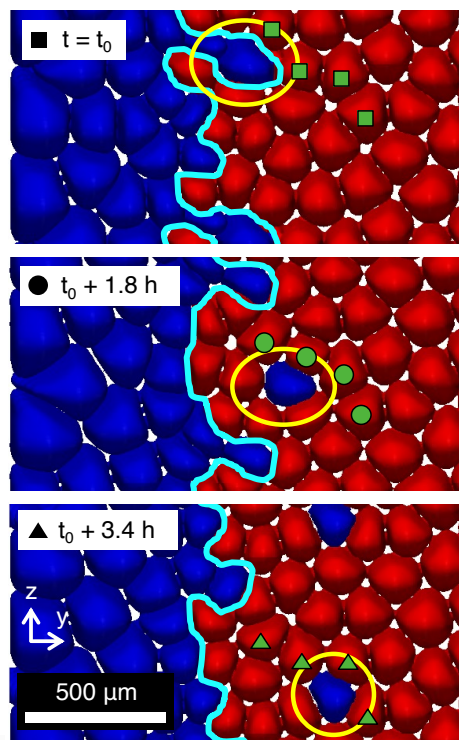
Jamgotchian et al., PRL (2001)



Experiment

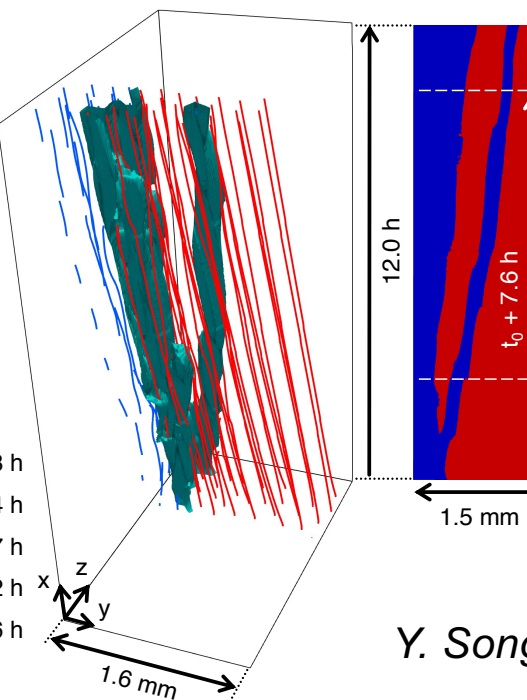


Simulation



Effects of grain boundary – A combined experimental and PF study

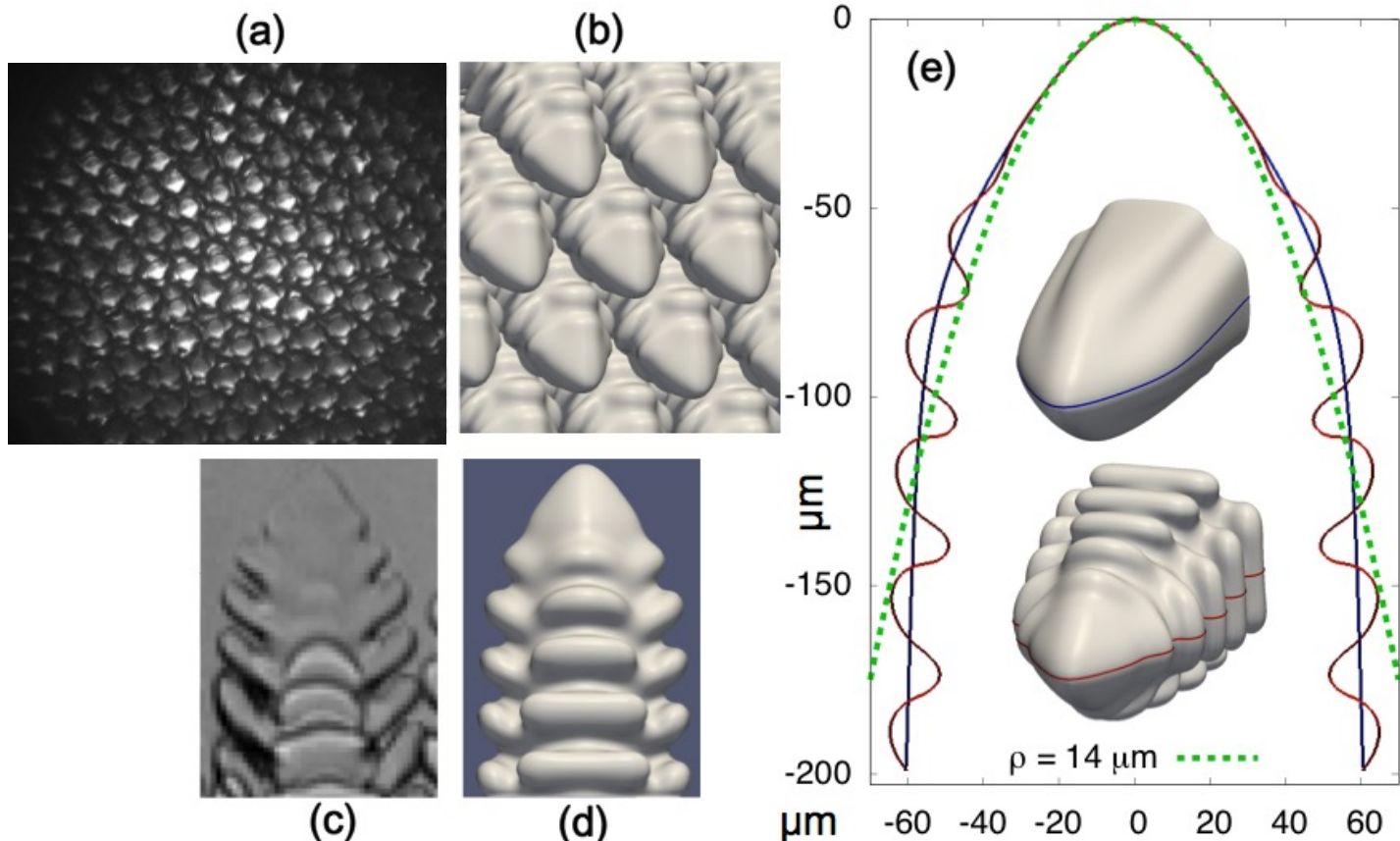
- Individual cells from one grain can invade a nearby grain of different misorientation, causing grains to interpenetrate and grain boundaries to adopt highly convoluted shapes.
- Agreement in the drifting dynamics of solitary cell between phase-field simulations and experiment (DSI).



Y. Song, F.L. Mota, D. Tourret, K. Ji, B. Billia, R. Trivedi, N. Bergeon, A. Karma, *Nat. Commun.*, in press

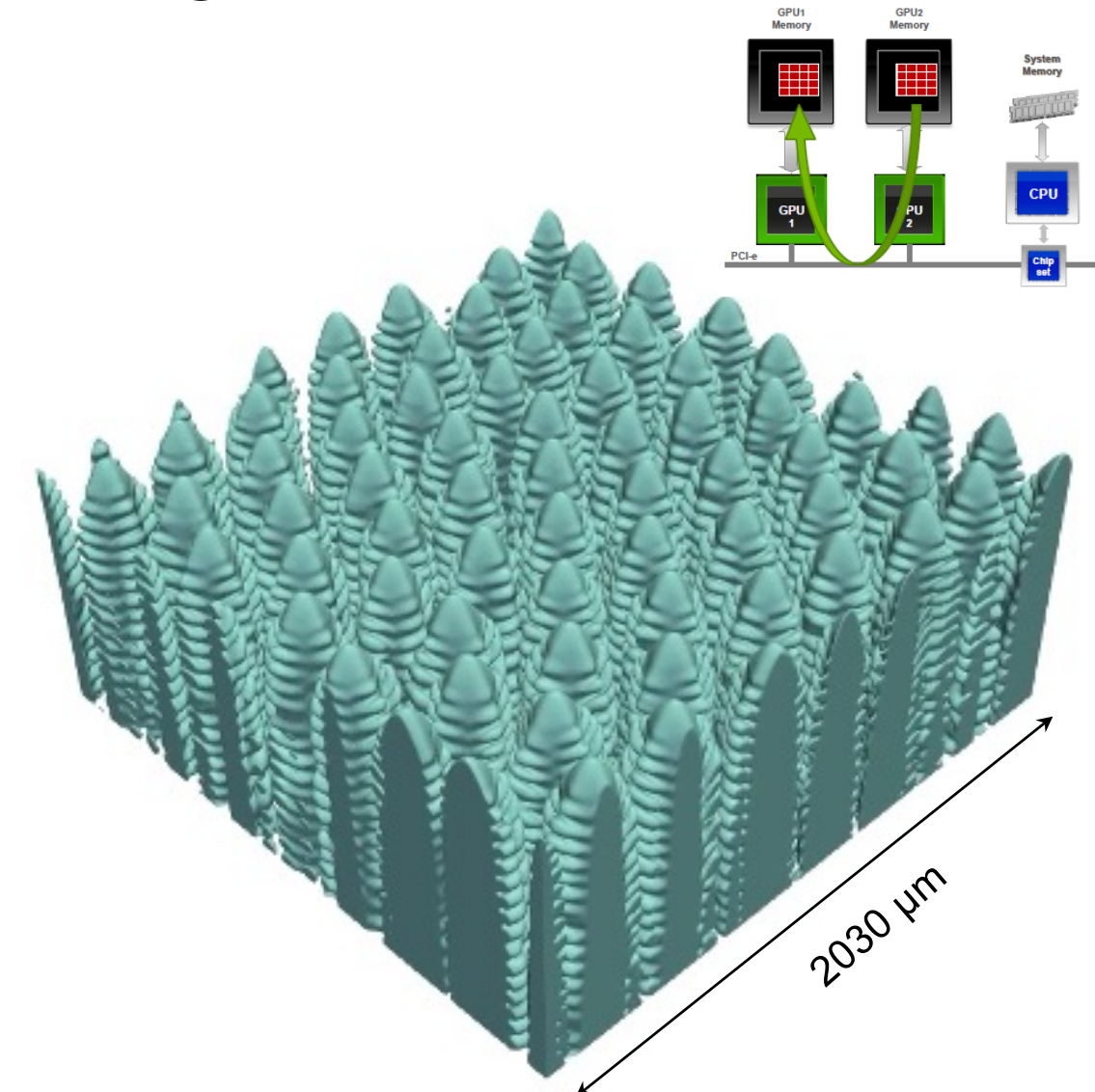
DSI-R Campaign: Increased alloy concentration

- Increase of concentration: dendrites at lower pulling rates
- Study of the formation of dendritic patterns

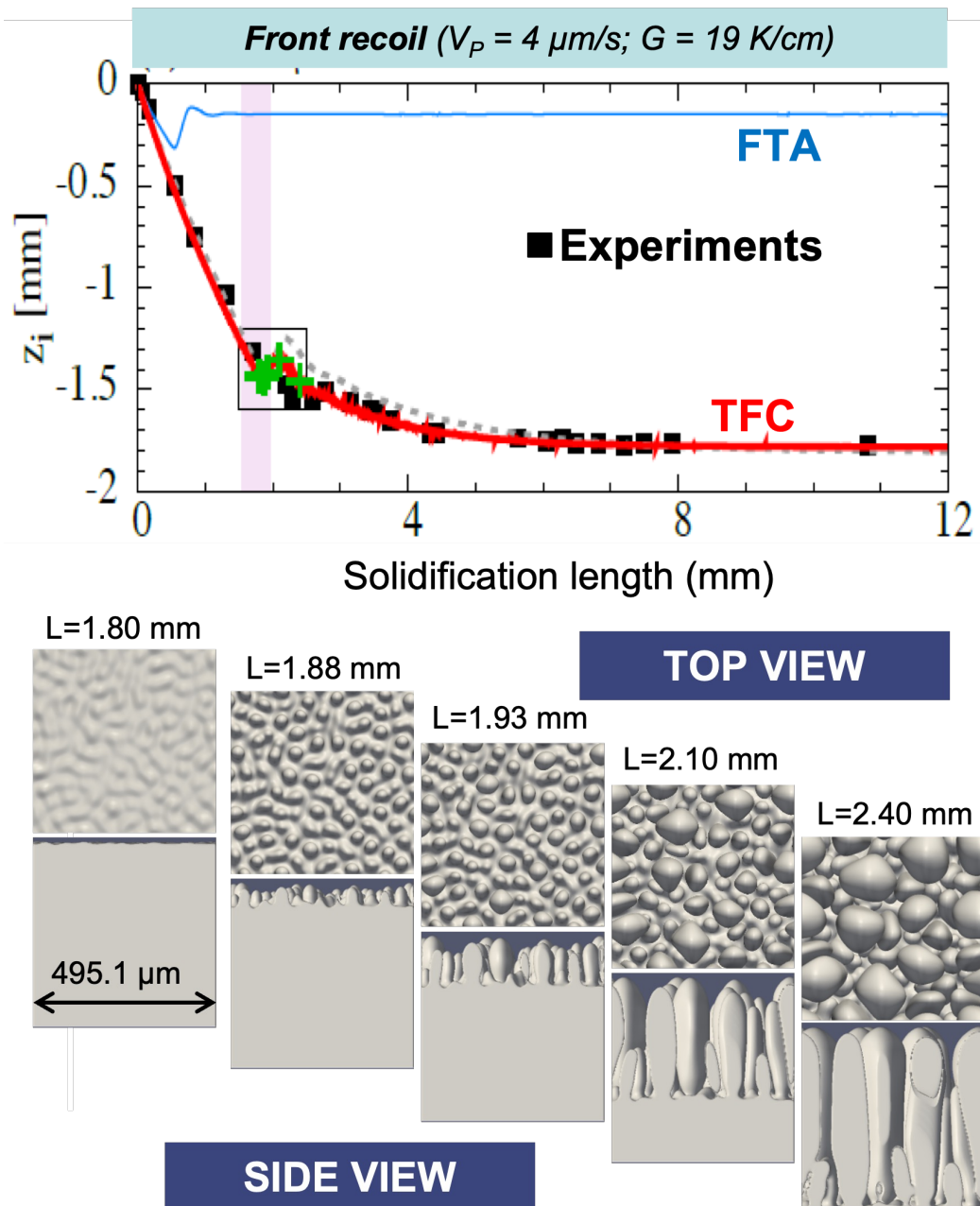


(a) SCN-0.46wt% camphor alloy, $V_p = 1.5 \mu\text{m/s}$, $G = 12 \text{ K/cm}$. (b-e) Preliminary results for SCN-0.5wt% camphor alloy ($V_p = 10 \mu\text{m/s}$, $G = 23 \text{ K/cm}$): (b) phase-field simulations of dendritic array; (c-d)

$G = 12 \text{ K/cm}$ and $C_0 = 0.46\text{wt\%}$ at $V = 1.5\text{--}3 \mu\text{m/s}$

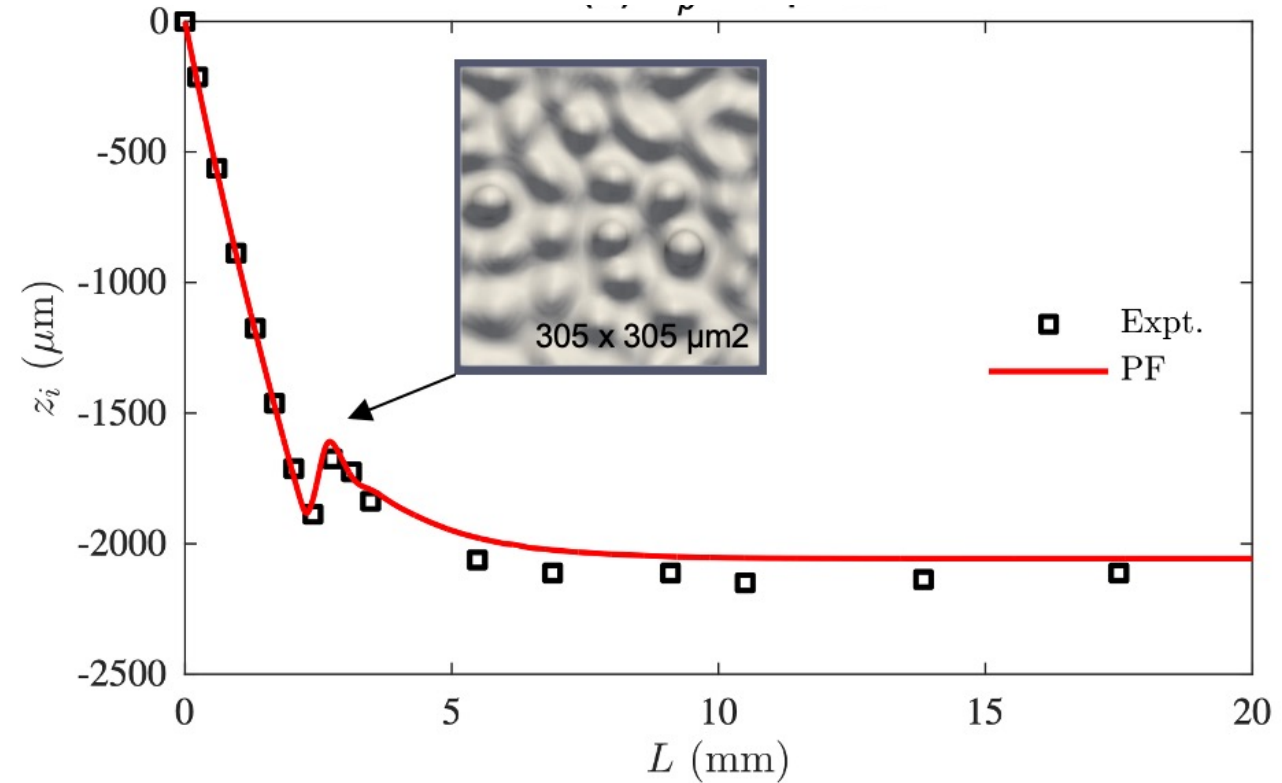


Solid-liquid interface recoil



Song et al. Acta Mater (2017)

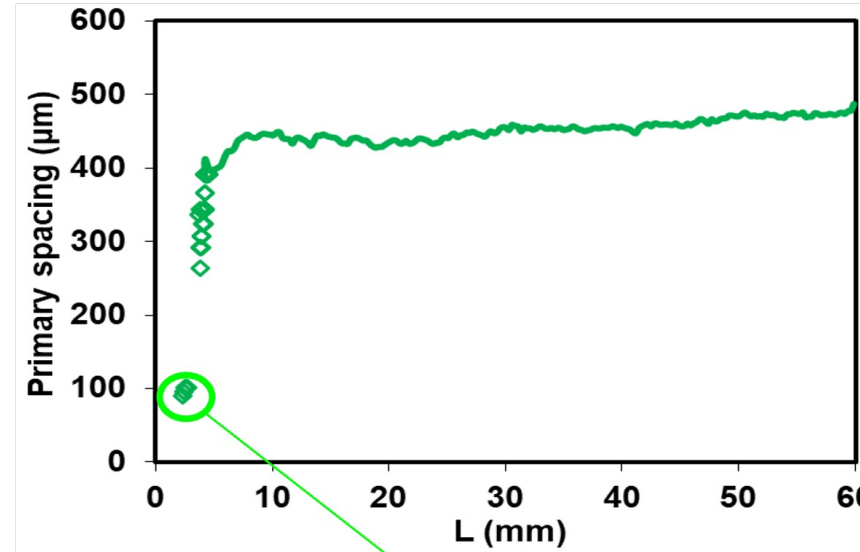
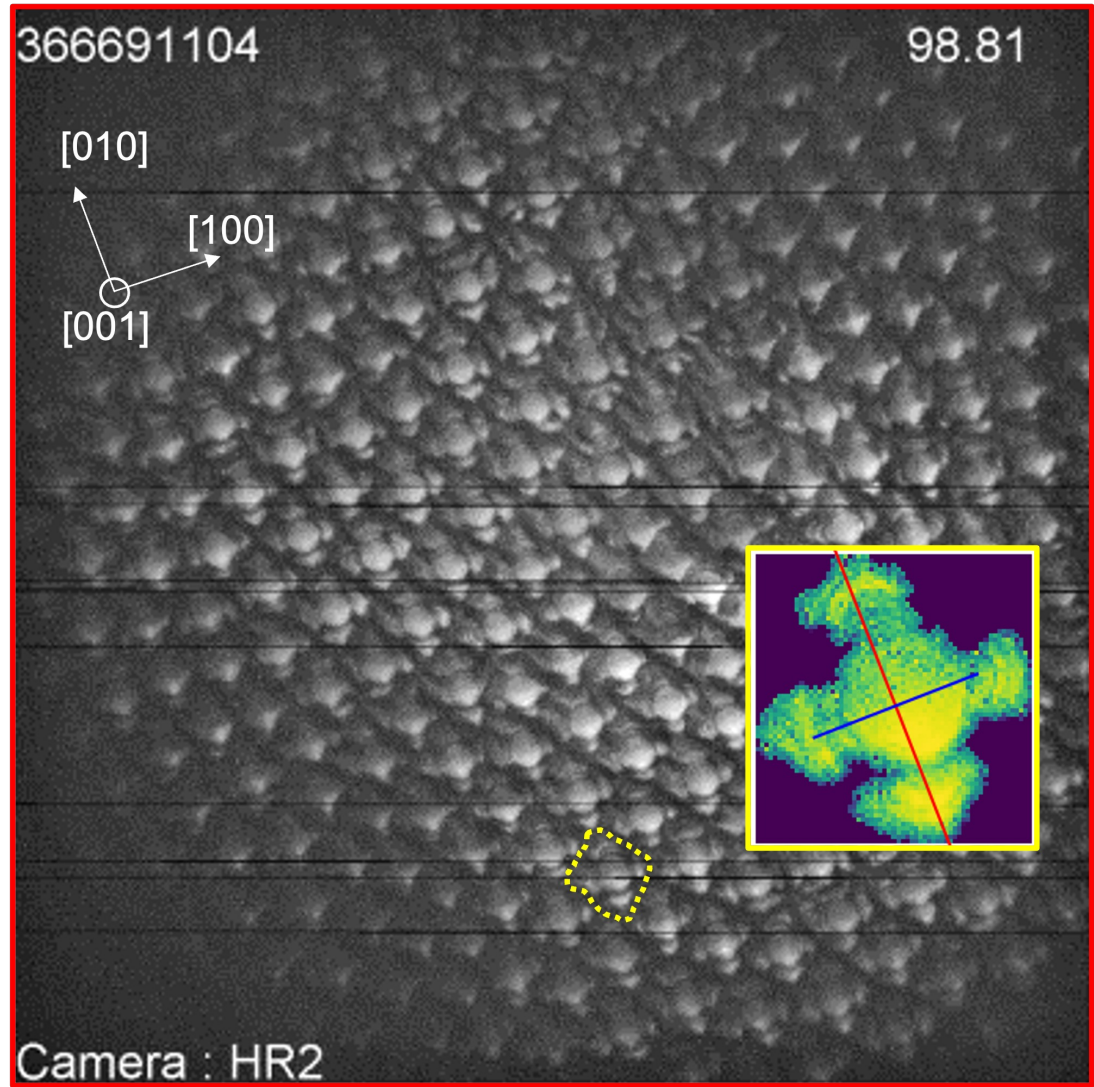
DSI-R: $V = 3 \mu\text{m/s}$ $G = 12 \text{ K/cm}$



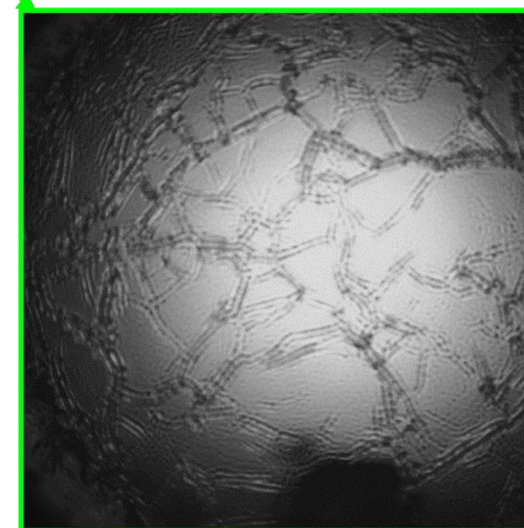
- The interface recoil in the phase-field simulation with latent heat diffusion agrees well to experiment.

Morphological instability

$$V = 3 \mu\text{m/s} \quad G = 12 \text{ K/cm}$$

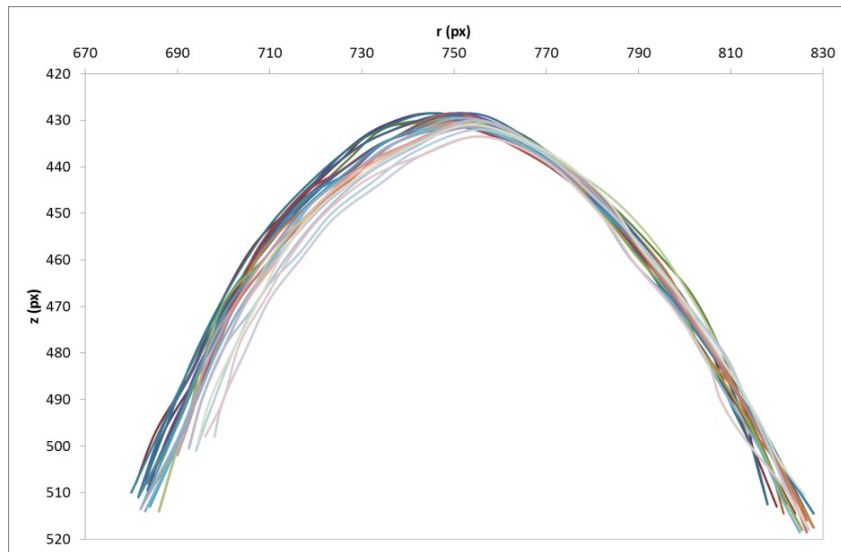


$$L = 2.4 \text{ mm}$$
$$\lambda_i = 91 \pm 10 \mu\text{m}$$

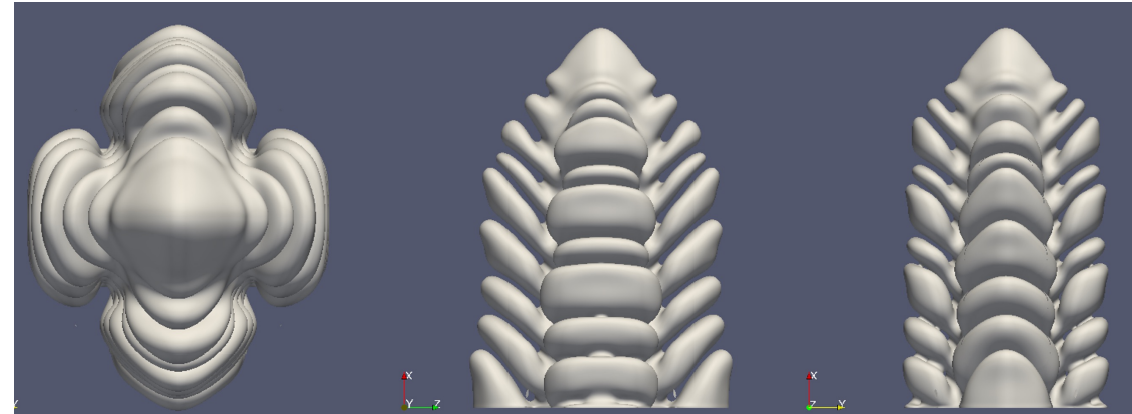
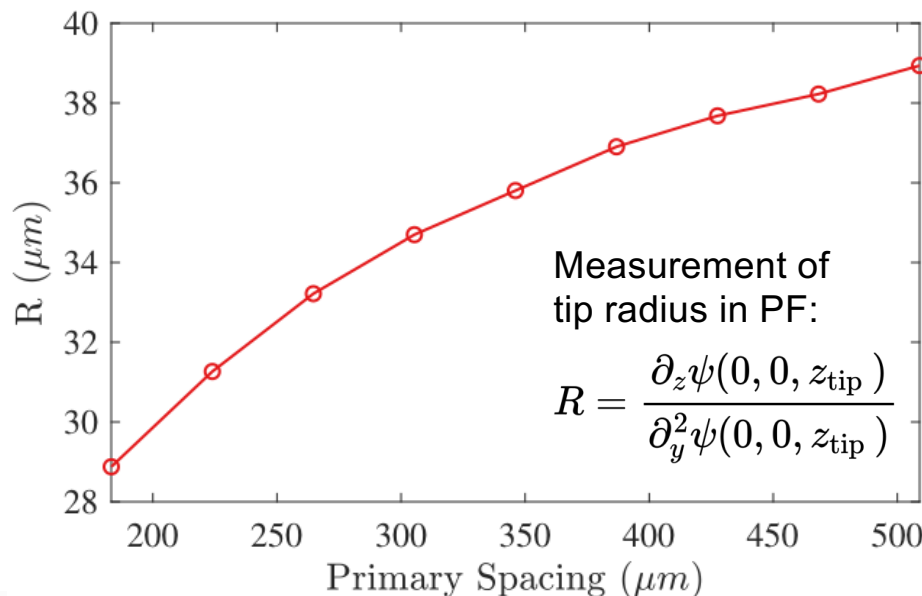
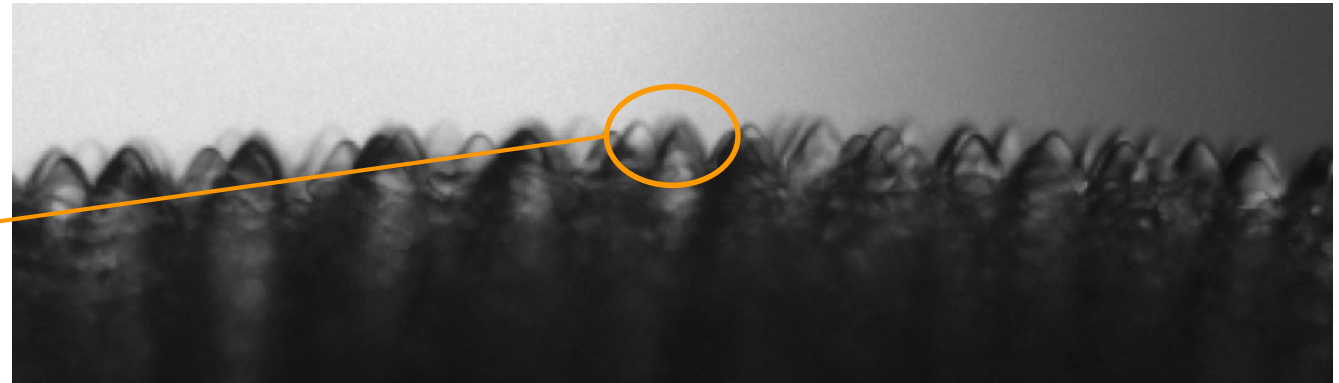


Initial $\lambda \sim 64 \mu\text{m}$ in phase-field simulation

Tip radius measurement

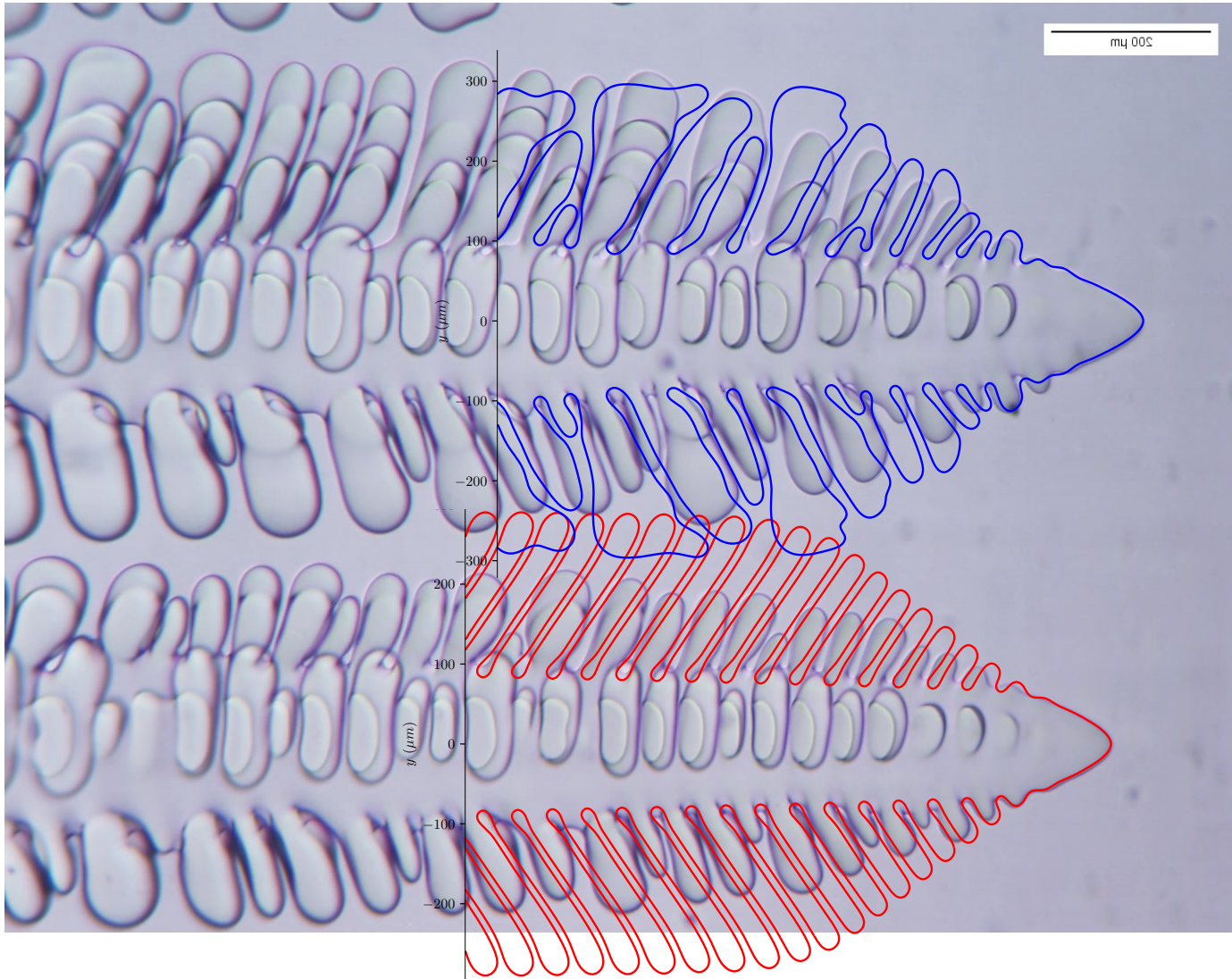


- The tip radius obtained in the PF simulation with (about 39 μm) agrees well to the experiment measurement of 39 μm .



Growth condition: $G = 12.5 \text{ K/cm}$ and $C_0 = 0.46\text{wt\%}$ at $V = 1.5 \mu\text{m/s}$

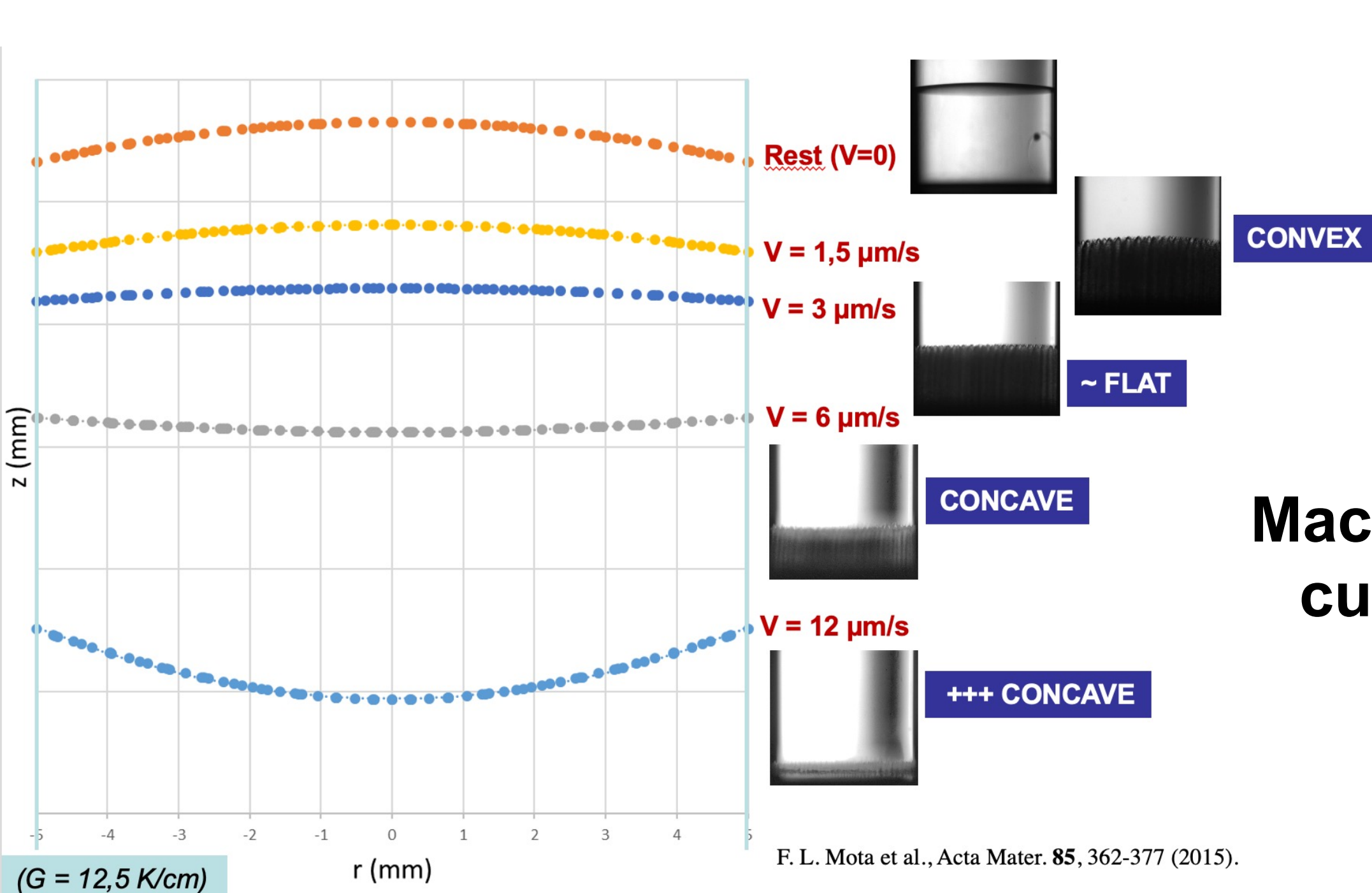
Comparison between PF simulation and experiment



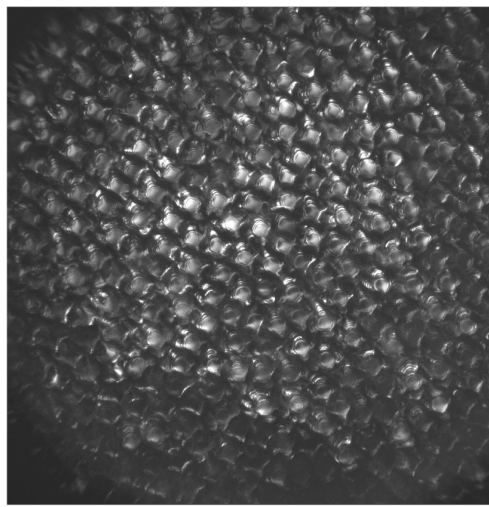
Ground-based experiment: $G = 12 \text{ K/cm}$ and $C_0 = 0.46\text{wt\%}$ at $V = 6 \mu\text{m/s}$

- The PF simulation can quantitatively model a dendrite tip, as validated by thin-sample experiment on the ground.
- The upper limit of primary spacing in the PF simulation is lower than experiments (a separate problem).
- Simulations with the oscillation of temperature around the tip. Promote sidebranching.

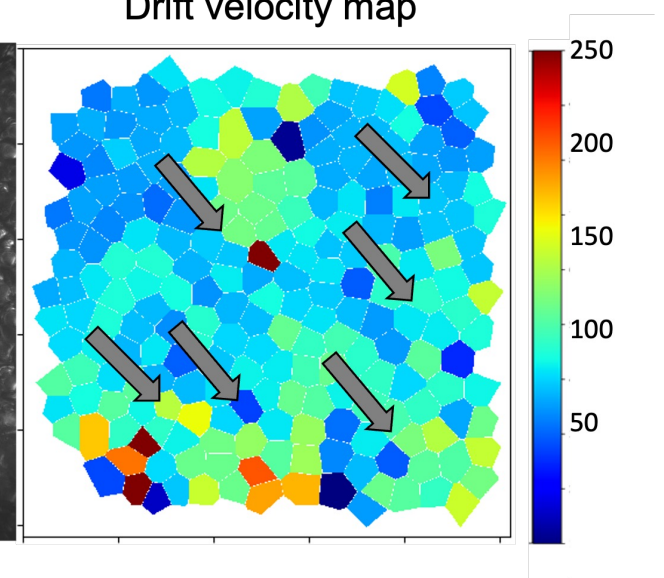
$$T(x) = G(x - V_p t) + A \cos(\omega t) e^{-\frac{|\vec{r} - \vec{r}_{tip}|^2}{b^2}}$$



FLAT - $V = 3 \mu\text{m/s}$

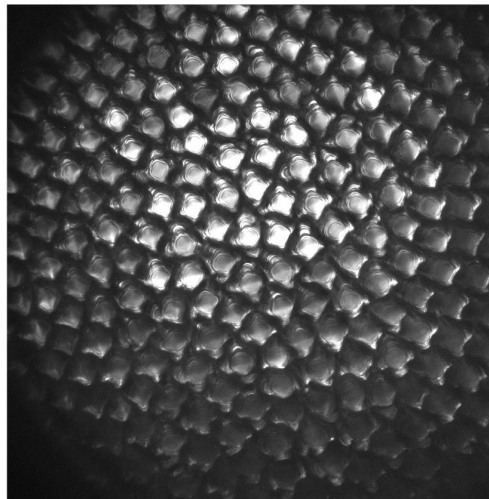


Drift velocity map

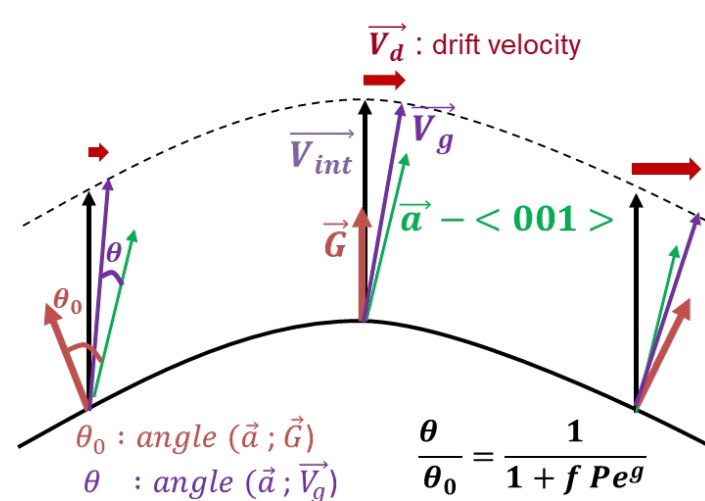
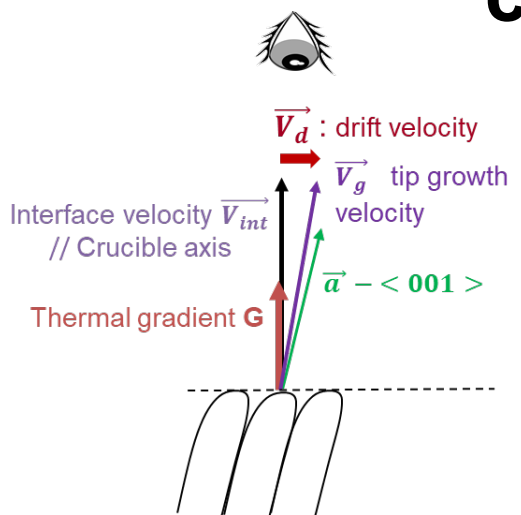


Drifting dynamics – misorientation and curvature

CONVEX - $V = 1,5 \mu\text{m/s}$



60 mm of growth, $G = 12,5 \text{ K/cm}$; $7.4 \times 7.4 \text{ mm}^2$



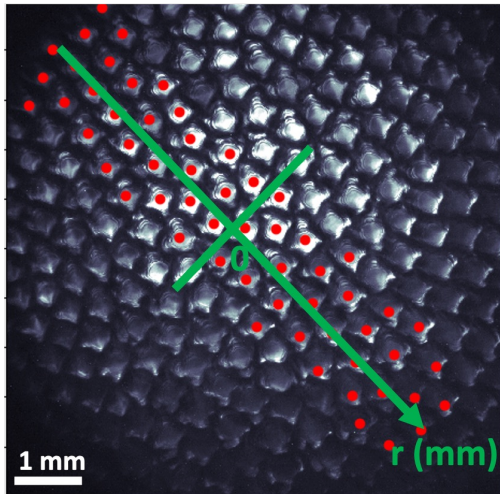
- Flat interface: Homogeneous drift of the dendritic pattern due to crystallographic misorientation.
- Macroscopic curvature is frequently observed, convex or concave, depending on velocity,
- Curvature modifies radially the misorientation angle => gradient of drift velocity

J. Deschamps et al. Phys. Rev. E **78**, 011605 (2008).
S. Akamatsu & T. Ihle, Phys. Rev. E **51**, 4751 (1995)

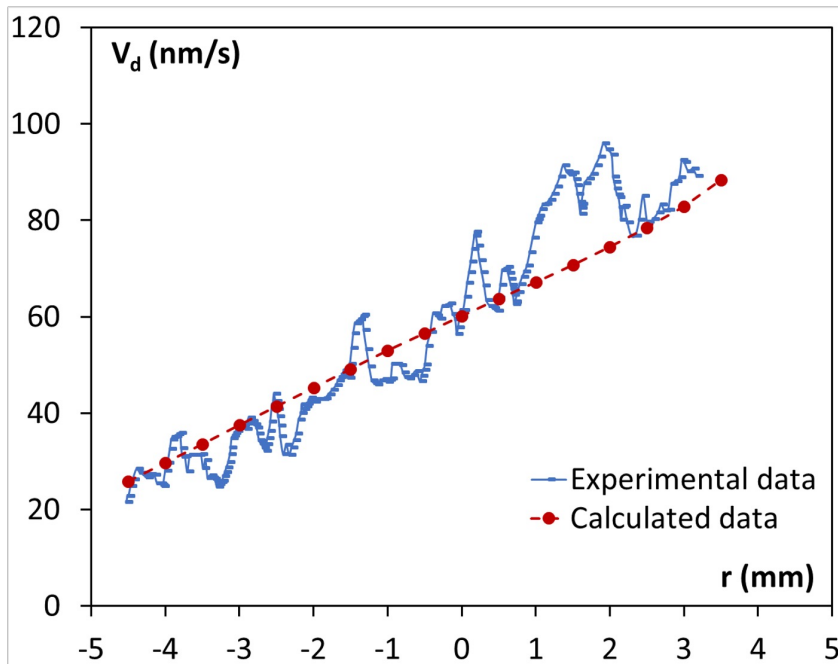


How does the drift velocity profile build ?

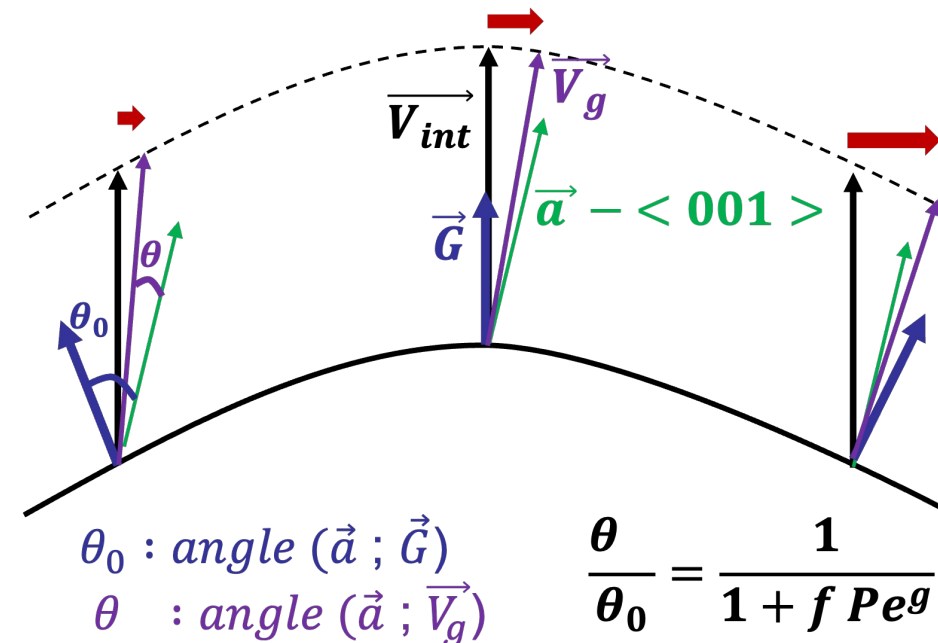
$V = 1,5 \mu\text{m/s}$



Drift velocity = $f(r)$



Curvature modifies radially the misorientation between the thermal gradient and the preferred crystallographic direction of growth

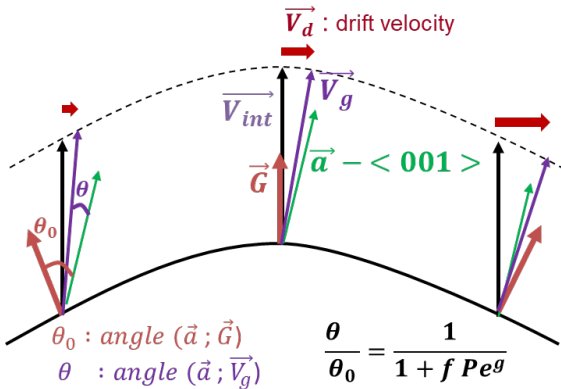


J. Deschamps et al. Phys. Rev. E 78 (1), 011605 (2008).

Validation of this analysis :

From EXP interface shape, determination of
V_drift_calculated as a function of r

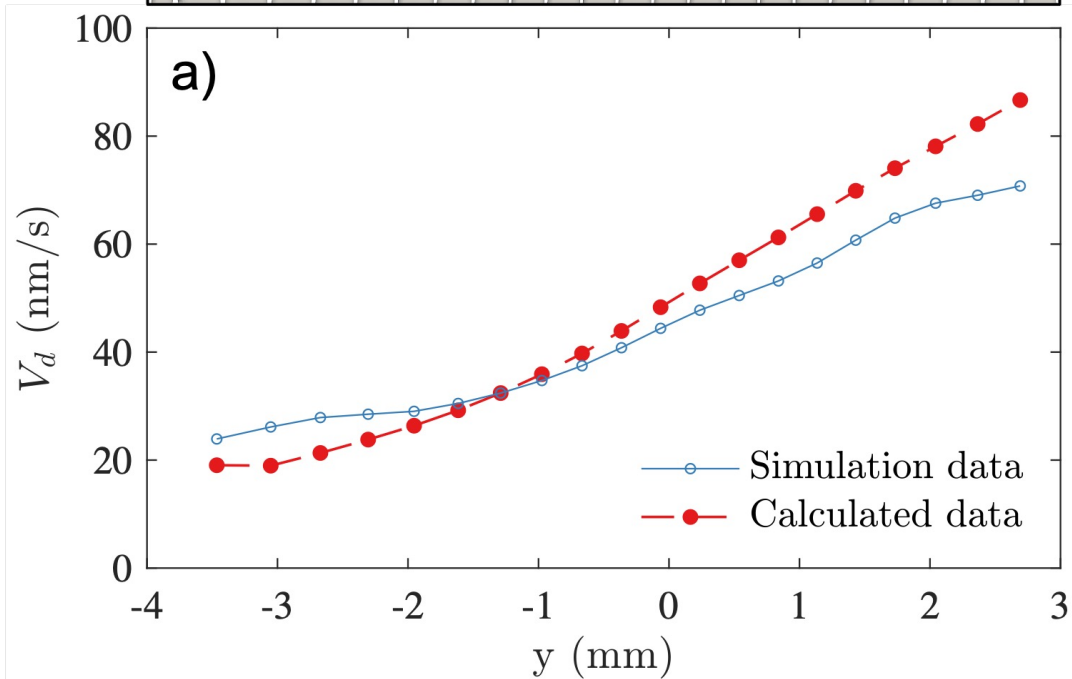
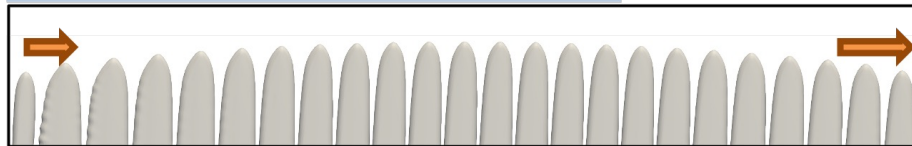
→ Good agreement with measurements



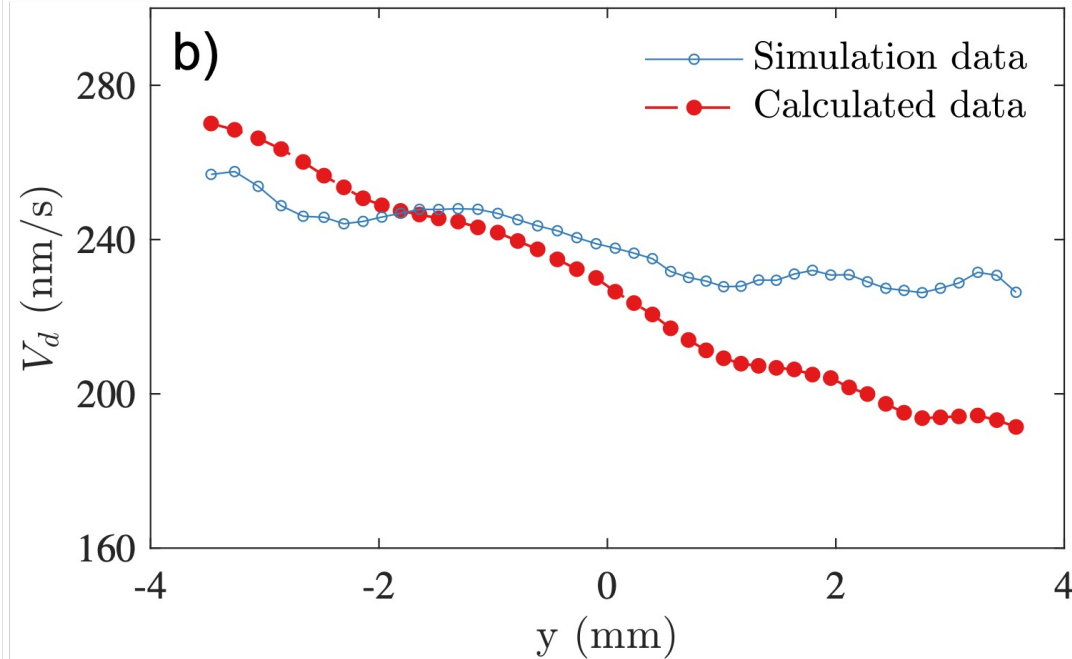
Effect of curvature on drifting velocity

- Velocity gradient: Curvature modifies radially the misorientation angle and causes a gradient of the cell drifting velocity.

$V = 1.5 \mu\text{m/s. Convex interface.}$



$V = 6 \mu\text{m/s. Concave interface.}$

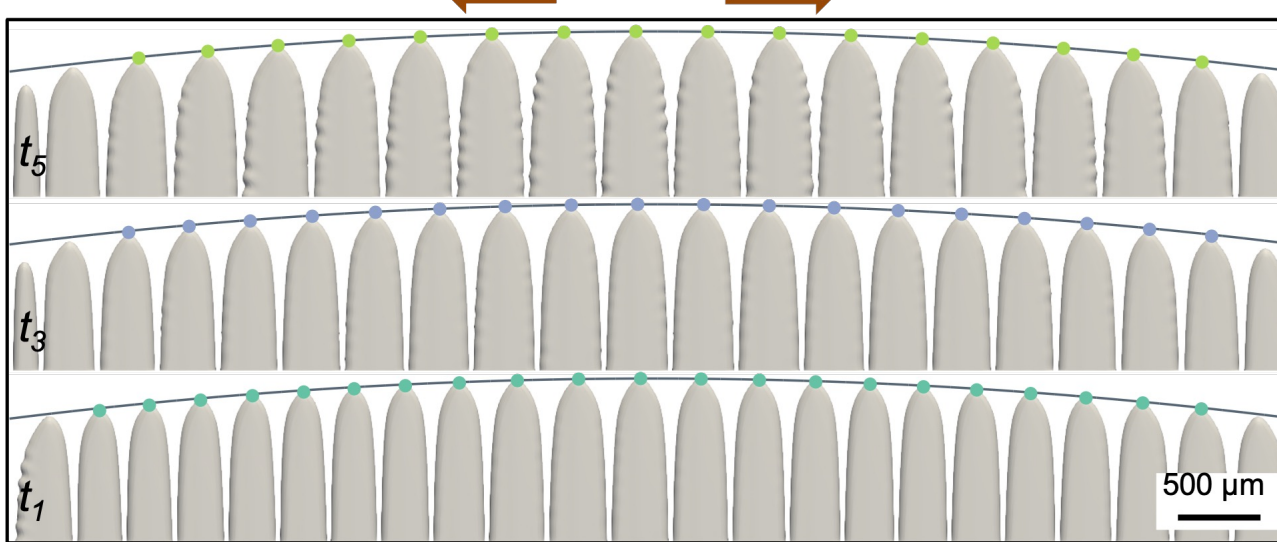


F.L. Mota, K. Ji et al. Acta Mat. (2023): 118849.

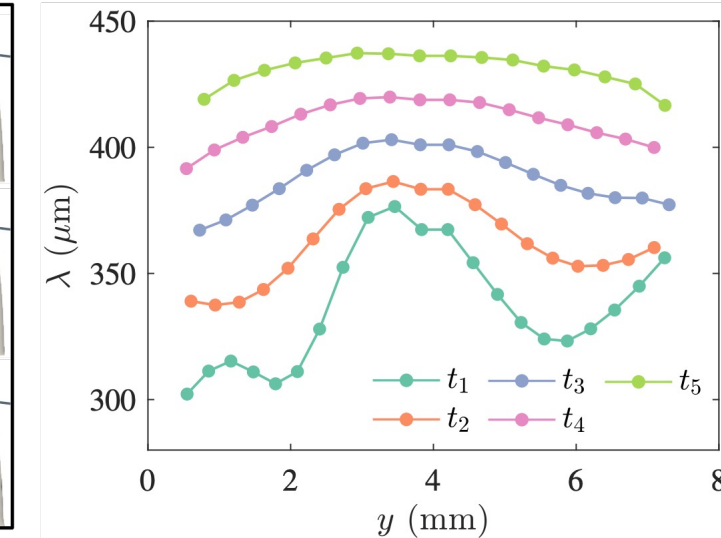
Spacing evolution due to curvature

- Dendrites drift towards the sample boundaries due to a convex curvature and towards the sample center due to a concave curvature. The spacing distribution evolves.

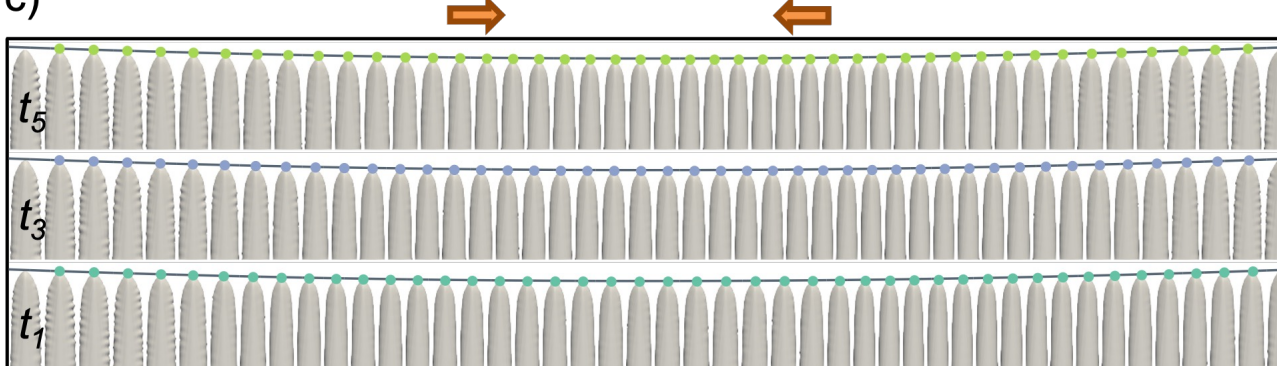
a)



b)

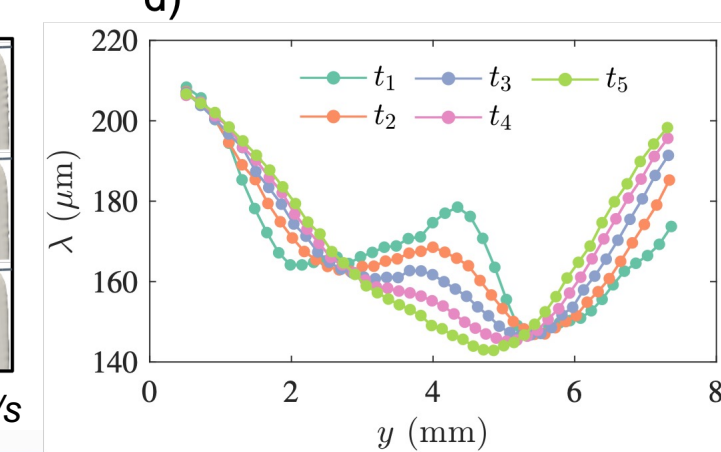


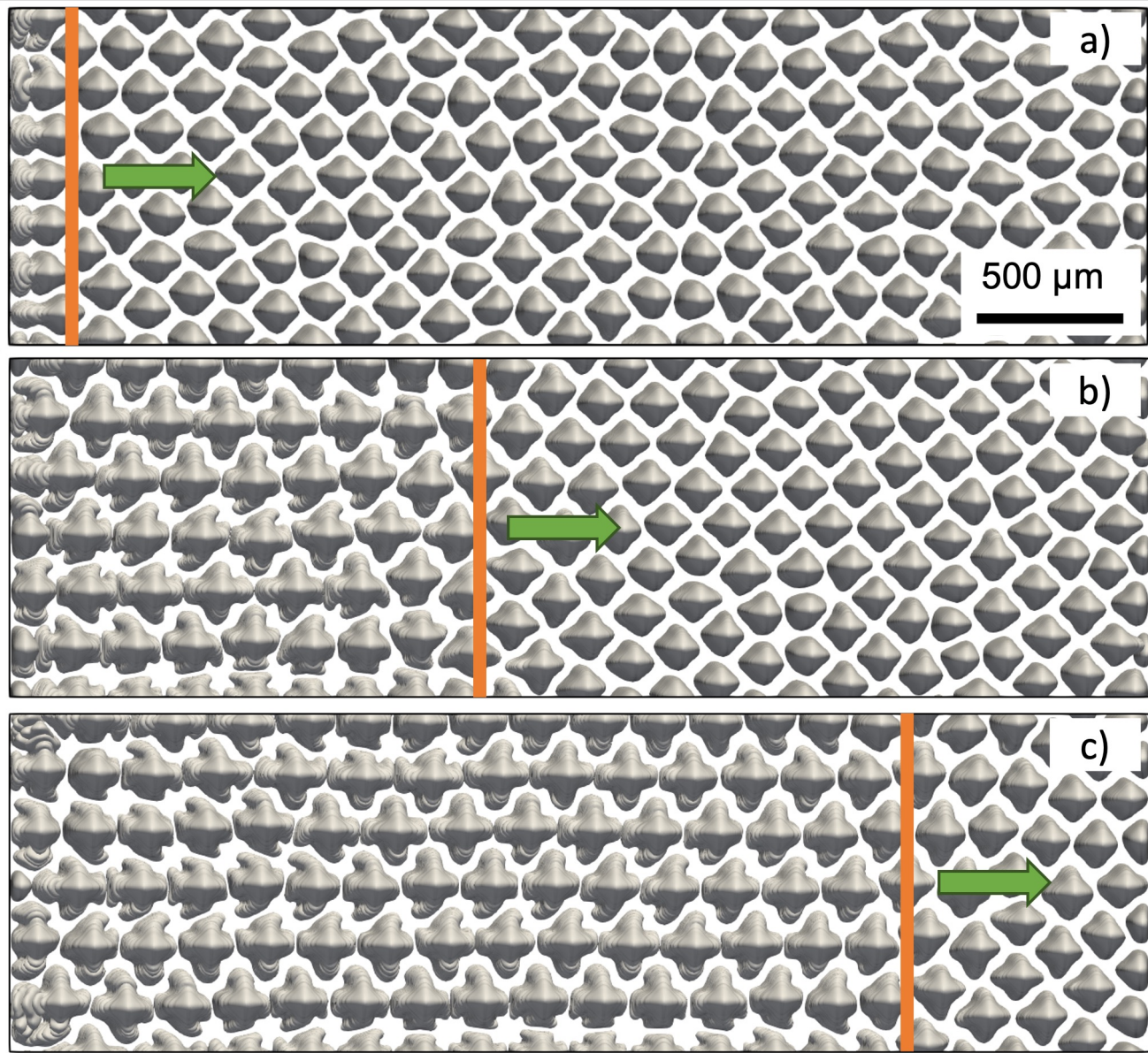
c)



SCN-0.46 wt% camphor alloy, $G = 12 \text{ K/cm}$, $V = 1.5$ (a)-(b) and 6 (c)-(d) $\mu\text{m/s}$

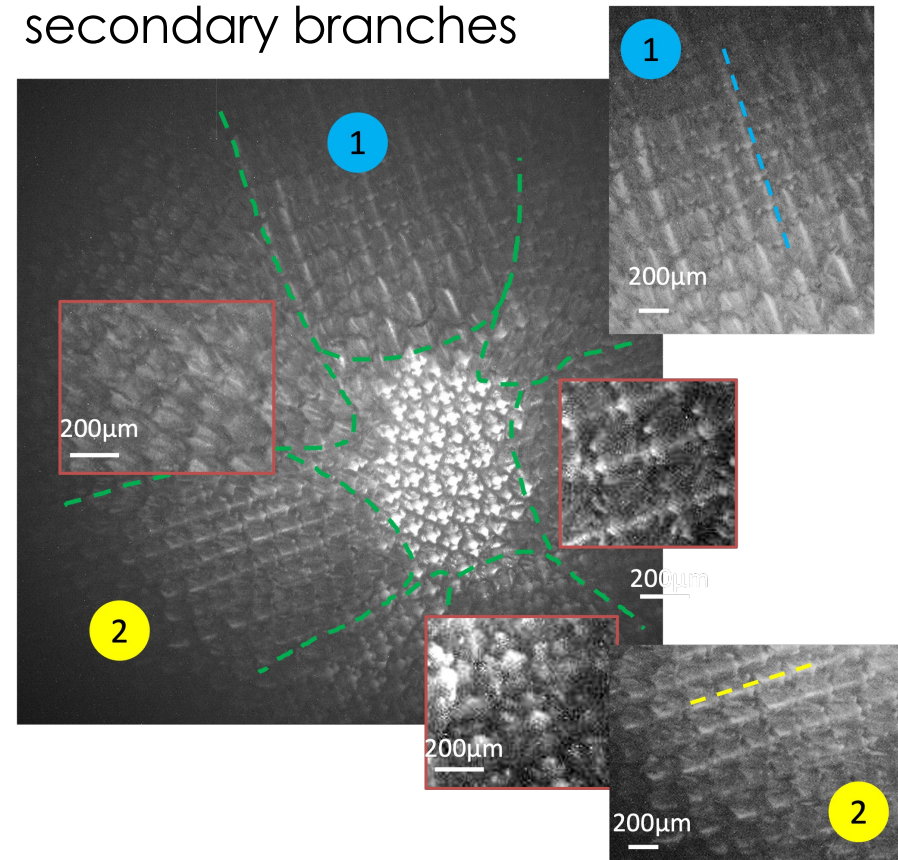
d)





→ **Stray-grains invasion**
 ⇒ induces disappearance of the well-oriented grain

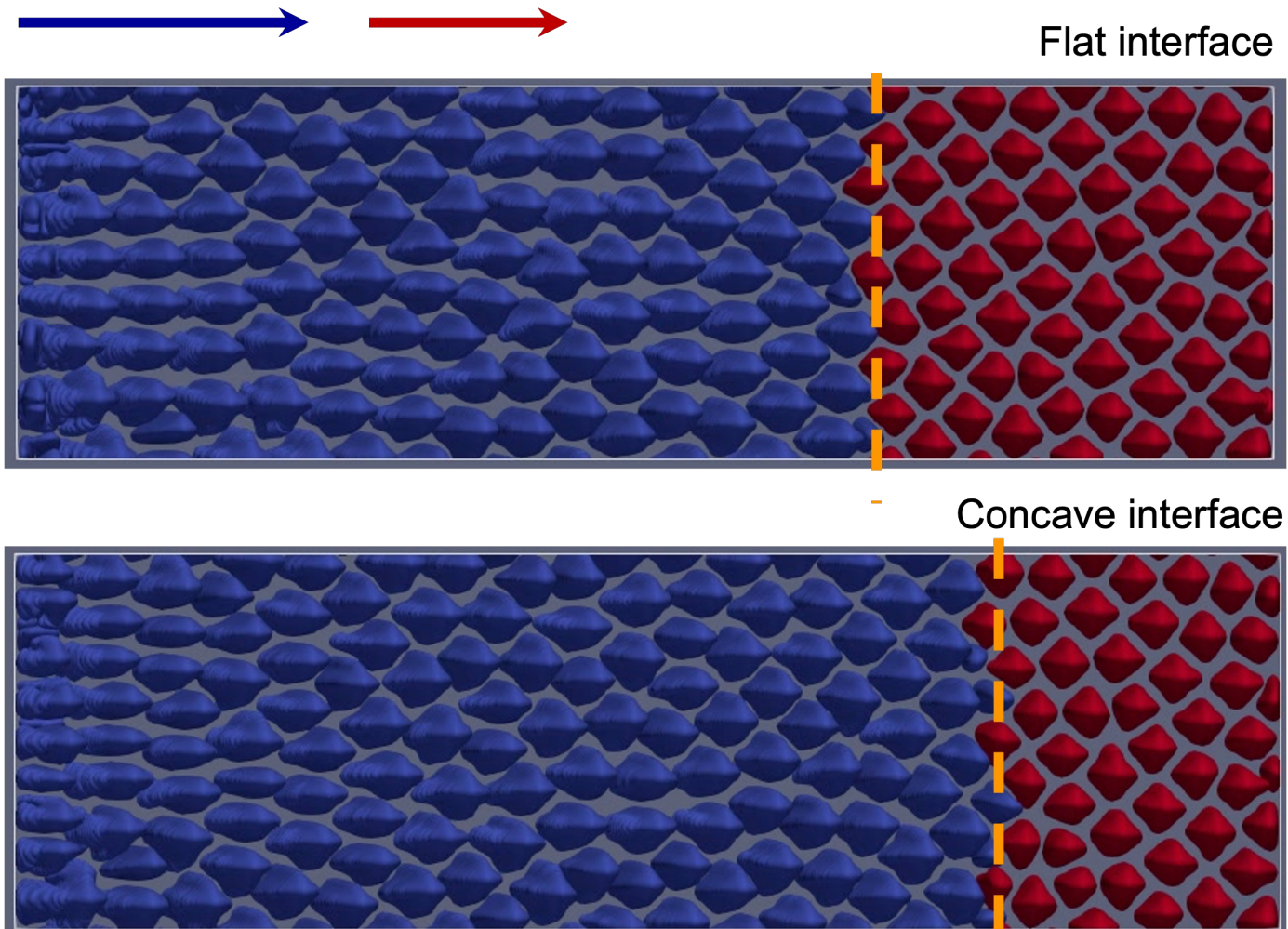
→ **Unusual pattern ordering**
 Alignment of dendrites // secondary branches



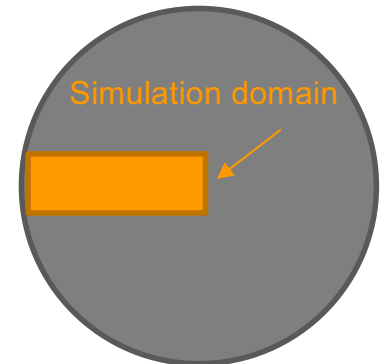
F.L. Mota, K. Ji et al. *Acta Mat.* (2023): 118849.

$G = 12 \text{ K/cm}$ and $C_0 = 0.46\text{wt\%}$ at $V = 6 \mu\text{m/s}$

Combined effects of macroscopic curvature and grain boundary



- The migration of a convergent grain boundary under the influence of a macroscopically concave interface.
- The grain boundary migrates faster under a concave interface compared with a flat interface.



$G = 12 \text{ K/cm}$ and $C_0 = 0.46\text{wt\%}$ at $V = 6 \mu\text{m/s}$; Misorientation **8.1 deg** for the blue grain and **2.7 deg** for the red grain

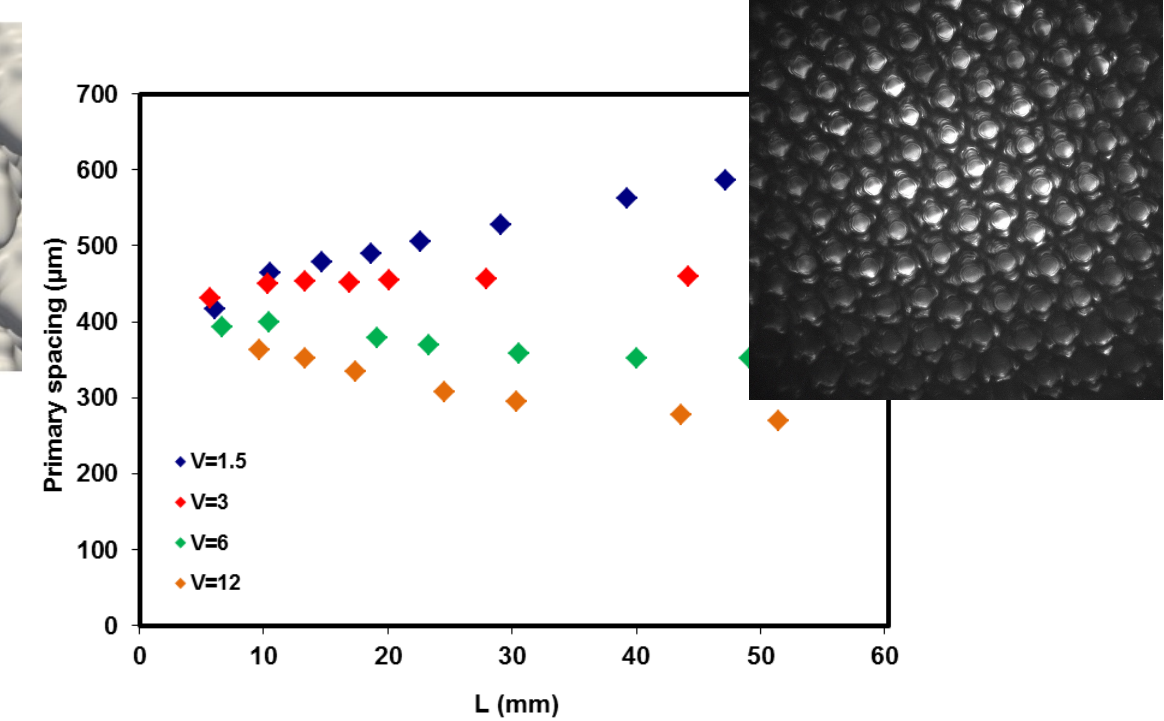
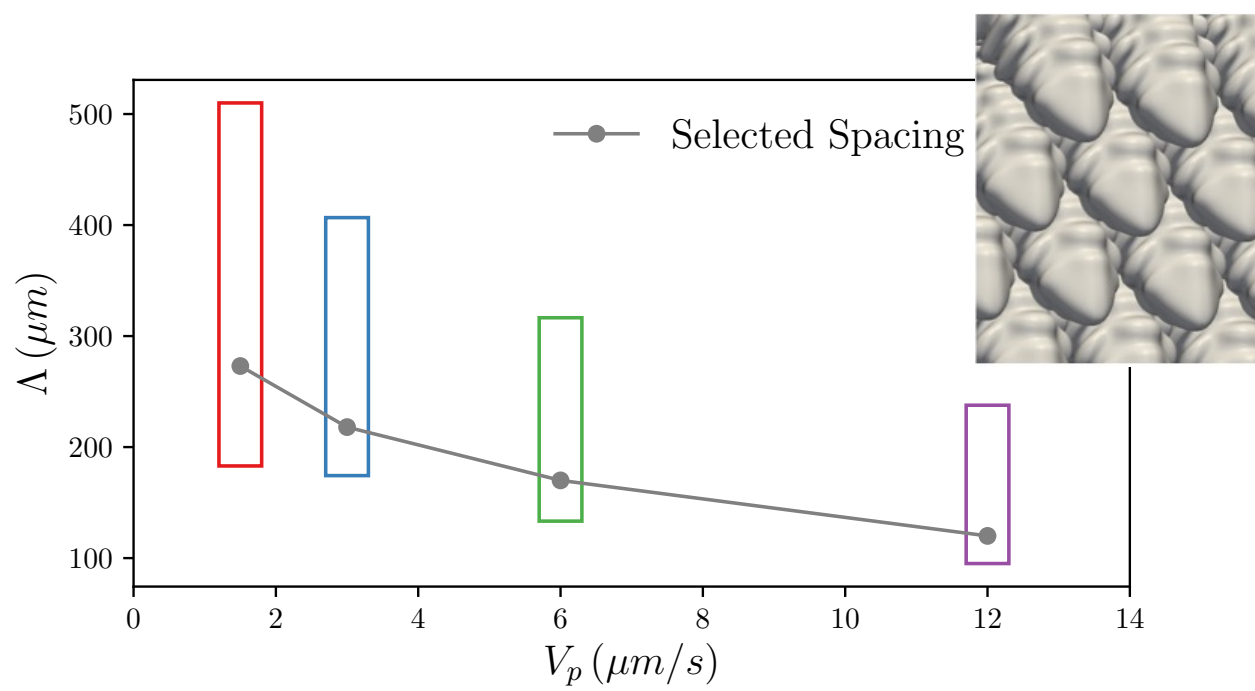
Summary

- Observation of dendritic patterns in **DSI-R** experiments and quantitative comparison with 3D phase-field simulations:
 - From the top view, the morphological instability and interface recoil.
 - From interferometry, the measurement of tip radius.
 - From the side view, macroscopic interface curvatures.
- Even a weak **macroscopic curvature** can create a gradient of lateral drifting velocity and affect the global behavior of growth interfaces.
- Microstructure evolution is affected by the **combined effects** of crystal misorientation, macroscopic curvatures, and grain boundary.



Outlook

- Quantitative comparison between PF simulation and DSI-R experiment.
- Investigate why the upper limit of primary spacing predicted by the phase-field simulation is lower than the experimental observation.
- Investigate the dendrite orientation transition.



Acknowledgement

Kaihua Ji, T. Lyons, A. Karma
Northeastern University



R. Trivedi
Iowa State University



This research is supported by NASA through awards NNX12AK54G, 80NSSC19K0135, and 80NSSC22K0664, and CNES through the MISOL3D project (Microstructures de SOLidification 3D).

F.L. Mota, M. Medjkoune, N. Bergeon
Aix-Marseillé Université



Marshall Space Flight Center



Thank you for your attention

